Exploring the role of organic matter accumulation on delta evolution

Jorge Lorenzo-Trueba,[1] Vaughan R. Voller,[1] Chris Paola,[2] Robert R. Twilley,[3] and Azure E. Bevington[3]

Received 9 January 2012; revised 28 May 2012; accepted 1 June 2012; published 20 July 2012.

[1] We explore the role of plant matter accumulation in the sediment column in determining the response of fluvial-deltas to base-level rise and simple subsidence profiles. Making the assumption that delta building processes operate to preserve the geometry of the delta plain, we model organic sedimentation in terms of the plant matter accumulation and accommodation (space made for sediment deposition) rates. A spatial integration of the organic sedimentation, added to the known river sediment input, leads to a model of delta evolution that estimates the fraction of organic sediments preserved in the delta. The model predicts that the maximum organic fraction occurs when the organic matter accumulation rate matches the accommodation rate, a result consistent with field observations. The model also recovers the upper limit for coal accumulation previously reported in the coal literature. Further, when the model is extended to account for differences in plant matter accumulation between fresh and saline environments (i.e., methanogenesis versus sulfate reduction) we show that an abrupt shift in the location of the fresh-salt boundary can amplify the speed of shoreline retreat.

Citation: Lorenzo-Trueba, J., V. R. Voller, C. Paola, R. R. Twilley, and A. E. Bevington (2012), Exploring the role of organic matter accumulation on delta evolution, *J. Geophys. Res.*, *117*, F00A02, doi:10.1029/2012JF002339.

1. Introduction

[2] A sediment mass balance as expressed by the Exner equation has proved to be a useful approach for (1) modeling the first order behavior during delta formation [*Swenson et al.*, 2000; *Capart et al.*, 2007, *Parker et al.*, 2008a, 2008b; *Lorenzo-Trueba et al.*, 2009; *Lorenzo-Trueba and Voller*, 2010], and (2) understanding how physical processes of delta growth contribute to delta restoration [*Kim et al.*, 2009; *Paola et al.*, 2011]. Such models involve a balance among sediment supply, sea level rise, and subsidence. To date, however, these models do not include the accumulation of organic matter in the delta plain. Coastal wetlands are among the most productive systems in the world [*Costanza et al.*, 1997; *Reddy and DeLaune*, 2008], and organic-rich sediment derived from plants typically represents a significant fraction of the sediment column [*Kosters et al.*, 1987, *Reddy and DeLaune*, 2008, *Törnqvist et al.*, 2008]. Moreover, plant matter accumulation has been identified as a potential control of marsh [*Morris et al.*, 2002; *Long et al.*, 2006; *Kirwan and Murray*, 2007; *Mudd et al.*, 2009] and delta evolution [*Fisk*, 1960; *Meckel et al.*, 2007; *Törnqvist et al.*, 2008; *van Asselen et al.*, 2009; *van Asselen*, 2011]. Thus, our objective here is to extend previous delta-growth geometric models [*Kim and Muto*, 2007; *Lorenzo-Trueba and Voller*, 2010] to include organic sedimentation in the system. The resulting model will be used to predict volume fraction of organics preserved in a delta plain as a function of accommodation and organic matter accumulation rates, and to explore the role of the fresh-salt groundwater boundary in determining the shoreline response to external forcing.

2. Organic Matter Accumulation

[3] Before describing the model, we first give a brief account of organic sedimentation. We assume that the primary source of organic sediment accumulation in the sediment column is from in situ plant production by coastal wetlands. Consequently, we neglect for now the accumulation of particle organic matter from other areas. We also note that the generation of organic sediments results from the excess of local plant productivity over decomposition rates [*Clymo*, 1983; *Moore*, 1989; *Richardson and Vepraskas*, 2001; *Reddy and DeLaune*, 2008]. Such excess—referred to henceforth as organic matter accumulation rate and denoted by P—is primarily controlled by the decomposition rate rather than productivity [*Moore*, 1989], i.e., organic matter accumulation increases where physical conditions serve to reduce decomposition processes. Organic matter decomposition involves a wide range of processes such as microbial

[1]Department of Civil Engineering, St. Anthony Falls Laboratory, University of Minnesota, Minneapolis, Minnesota, USA.
[2]School of Earth Sciences, St. Anthony Falls Laboratory, University of Minnesota, Minneapolis, Minnesota, USA.
[3]Department of Oceanography and Coastal Science, Louisiana State University, Baton Rouge, Louisiana, USA.

Corresponding author: J. Lorenzo-Trueba, Department of Civil Engineering, St. Anthony Falls Laboratory, University of Minnesota, Minneapolis, MN 55414, USA. (loren153@umn.edu)

0148-0227/12/2012JF002339

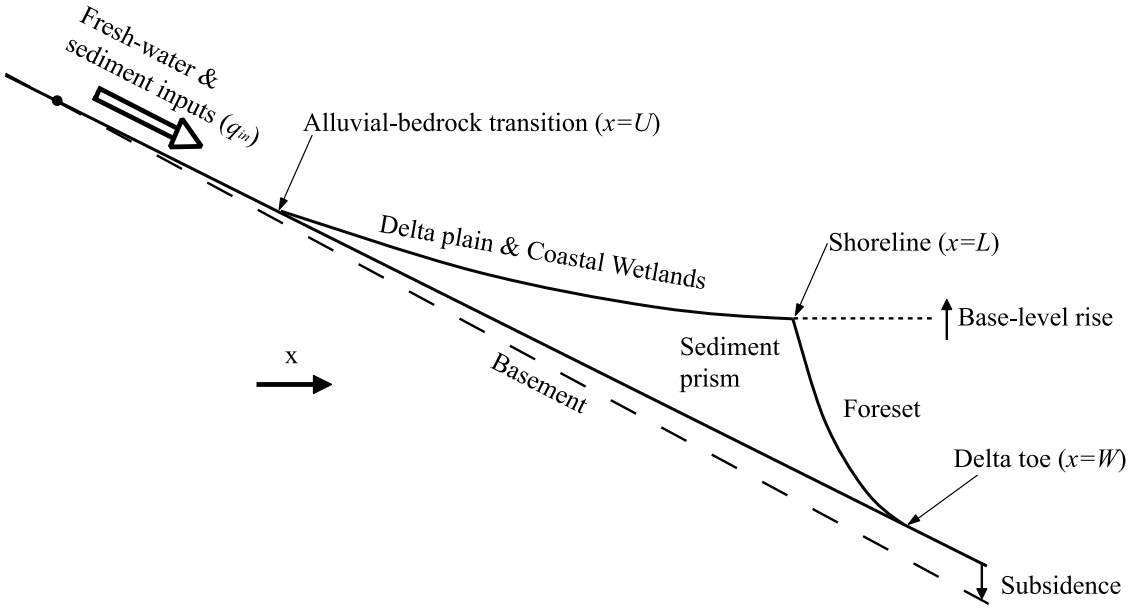

Figure 1. Typical delta profile.

activity (carried out by microorganisms such as fungi and bacteria) or fire oxidation, and is generally separated into aerobic and anaerobic components [*Richardson and Vepraskas*, 2001; *Reddy and DeLaune*, 2008]. Under aerobic conditions, due to enhancement microbial growth [*Portnoy*, 1999; *Gambolati et al.*, 2006], the decomposition is of the same order as production, and as such the organic matter accumulation is close to zero. In contrast, under anaerobic conditions, like those often found in deltaic wetlands, organic matter accumulation is significant [*Kosters et al.*, 1987; *Richardson and Vepraskas*, 2001, *Reddy and DeLaune*, 2008]. In such anaerobic environments the organic matter accumulation is controlled by the presence of sulfate among other factors. In saline environments sulfate reduction is the major form of anaerobic decomposition [*Howarth and Hobbie*, 1982; *Senior et al.*, 1982; *Howarth*, 1984; *Capone and Kiene*, 1988]. In fresh water environments, however, the amount of sulfate is limited and methanogenesis is the predominant decomposition mechanism [*Capone and Kiene*, 1988]. Since sulfate reduction is energetically superior to methanogenesis [*Capone and Kiene*, 1988; *Portnoy and Giblin*, 1997; *Ibañez et al.*, 2010], we expect a larger organic production rate in fresh systems compared to saline, a situation often observed in field studies [*Portnoy and Giblin*, 1997; *Portnoy*, 1999; *Ibañez et al.*, 2010]. Furthermore, this imbalance between the nearshore saline and the inland fresh regions has been observed in stratigraphic studies of different deltaic environments [*Kosters et al.*, 1987; *Kosters and Suter*, 1993; *Staub and Esterle*, 1994].

3. Model Description

[4] The task now is to quantify and incorporate organic sedimentation into a delta growth model. In Figure 1 we present a sketch of a cross-section of a river delta. The system is fed by fresh water and sediment from the river system, and evolves on top of the basement under conditions of sea level rise and subsidence. The key geometric feature in this system is the deposited sediment prism. This shape is bounded below by the basement, and from above by the subaerial delta plain and the subaqueous foreset. The delta plain is delimited by the shoreline and the alluvial-basement transition, and the foreset by the shoreline and the delta toe. The movements of these three geomorphic boundaries (alluvial-basement transition, shoreline and delta toe) define the evolution of the delta in cross-section.

[5] Within the system shown in Figure 1, the sediment volume per unit width in the prism V is determined by the external bulk sediment input from the river system q_{in}, and the rate of accumulation of plant matter within the delta plain. River sediment inputs q_{in} are either trapped in the delta plain, which results in shoreline aggradation, or bypass the delta plain and deposit in the subaqueous foreset, which drives shoreline progradation. The partitioning of sediment between the delta plain and the foreset is controlled by the geometry of the deltaic prism. To first order we assume that all the sediment input from the river is trapped within the deltaic prim, but we recognize that a significant fraction might be transported beyond the delta toe [*Allison et al.*, 1998; *Blum and Roberts*, 2009]. If we define $\chi(x, t)$ to be the thickness of organic as opposed to inorganic sediments at each location, the volume of sediments in the prism, at time t, is then given by

$$V = \int_0^t q_{in}\, dt + \int_U^W \chi\, dx \tag{1}$$

where the second term on the right is an integration over the sediment prism in Figure 1 with $x = U$ the location of the alluvial-basement transition and $x = W$ the location of the delta toe.

[6] In this initial modeling exercise we assume that q_{in} is constant, and that the in situ production of organic matter in

the subaqueous foreset (between the shoreline L and the delta toe W) is negligible. We recognize, however, that in real systems the burial of organic sediments in the shelf could be significant [*Bianchi*, 2011; *Sampere et al.*, 2011], and future (and more elaborate) versions of the model will explore the potential consequences of this process on delta evolution. Under these conditions, it follows from (1) that the rate of change of the prism sediment volume $\dot{V} = dV/dt$ can be written as

$$\dot{V} = q_{in} + \int_U^L \nu_{org} dx \tag{2}$$

Here we recognize that the sediment column has zero height at the alluvial-basement transition and toe, and have defined $v_{org}(x) = \partial\chi/\partial t$ as the rate of organic sedimentation at any location x in the delta plain.

[7] To advance from equation (2) we simplify the geometry in Figure 1. First we note the basement β and foreset ψ slopes are rather constant in natural systems [*Blum and Törnqvist*, 2000; *Muto and Steel*, 2002; *Blum and Roberts*, 2009]. Thus, following previous modeling efforts [*Swenson et al.*, 2000; *Lorenzo-Trueba et al.*, 2009; *Lorenzo-Trueba and Voller*, 2010; *Paola et al.*, 2011], we assume a linear foreset with constant slope ψ and a linear basement with constant slope β. *Kim and Muto* [2007] have extended this simplification by assuming a linear profile, with slope γ, for the delta plain as well. In an exact mathematical analysis, based on a diffusion treatment for sediment transport, *Lorenzo-Trueba and Voller* [2010] explicitly verified the accuracy of this approach when the slope ratio $\gamma/\beta \leq 0.7$; a condition often seen in costal wetland systems of interest here [*Blum and Törnqvist*, 2000; *Muto and Steel*, 2002]. As such, we adopt this linear shape preserving assumption in the current work which allows us to simplify the geometry to that shown in Figure 2a.

[8] We consider two scenarios: base-level rise and differential subsidence. In the base-level rise case we assume the subsidence, the sum of crustal processes and compaction, to be spatially uniform. In contrast, in the differential subsidence scenario the subsidence rate increases linearly seawards from a pivot location (see Figure 1). We assume that in a Holocene context this pivot location is located approximately at the landward limit of the onlap, which is ~100 km upstream from the shoreline [*Blum and Törnqvist*, 2000]. Thus, the main ingredients in a model for delta evolution are (1) the interplay between the rate of change of the sediment per unit width in the prism $\dot{V}$, and (2) either the combination of sea level and subsidence expressed as a base-level rise $\dot{Z}$, or the pivot subsidence rate $\dot{\beta}$. The base-level Z and basement slope β are defined as

$$Z = Z_0 - \dot{Z}t \tag{3a}$$

$$\beta = \beta_0 + \dot{\beta}t \tag{3b}$$

where Z_0 and β_0 are the base-level and basement slope at $t = 0$. The origin is chosen to be located on the basement, at one characteristic basin length distance ℓ landwards from the initial shoreline location, and with x positive in the seaward direction and z positive downward (Figure 2a). As characteristic basin length we choose the distance from the landward limit of the onlap to the shoreline (i.e., $\ell \sim 100$ km [*Blum and Törnqvist*, 2000]). In this way, in the pivot scenario the origin coincides with the pivot location. For completeness, in Figure 2b, we also show the realization of the concept of the shape preservation under a situation in which, at a point in time, the sediment supply and accumulation cannot sustain a shoreline advance resulting in an abandonment of the foreset and a shoreline retreat.

[9] Taking account of our shape preserving assumption we can constrain the rate of organic sedimentation in (2) by

$$v_{org} = \min(A, P) \tag{4}$$

where P is the organic matter accumulation rate — fully discussed in the previous section—and A the rate of accommodation due to base-level rise (i.e., $A = \dot{Z}$) or differential subsidence (i.e., $A = \dot{\beta}x$). The model in (4) says that, in situations where the organic matter accumulation rate outstrips the rate of accommodation, i.e., $P > A$, the organic excess—to preserve shape—is either rapidly decomposed via aerobic respiration (i.e., oxidation) or eroded away. Under these conditions, an increase in accommodation rate A would lead to an increase in organic sedimentation v_{org}, which is consistent with previous formulations and field observations [*Morris et al.*, 2002; *Mudd et al.*, 2009]. On the other hand, if the organic matter accumulation rate cannot keep up with the accommodation rate, i.e., $P < A$, it is assumed that the shape is preserved by filling in the shortfall with the available inorganic sediment supply. In this case, an increase in accommodation rate A would not lead to an increase in organic sedimentation v_{org}, and if the inorganic sediment is insufficient there is potentially a retreat in the shoreline location.

[10] Note that equation (4) implies that spatial changes in the inorganic sedimentation rate $v_{in}(x, t)$ are a function of the space left for deposition by the organic sediments, i.e., max (A-P, 0). For instance, under the base-level rise scenario, if we assume that the organic matter accumulation rate P decreases downstream (as discussed in section 2) and is always less than the accommodation rate $\dot{Z}$, then inorganic sedimentation rate must increase downstream in order to satisfy our shape preservation assumption. In the first instance, however, we assume a constant value for the organic accumulation rate P (an assumption that will be relaxed later). In this way, for the base-level rise case we can use (4) to evaluate the integral on the right hand side of (2) and arrive at

$$\dot{V} = q_{in} + (L - U) \cdot \min(\dot{Z}, P) \tag{5a}$$

and the differential subsidence case becomes

$$\dot{V} = q_{in} + \int_U^L \min(\dot{\beta}x, P) dx \tag{5b}$$

with initial conditions $V = 0, L = 1$, and $U = 1$. For given values of P, q_{in} and A, the coupling of the solution of (5) to the geometric features in Figure 2 will fully realize a model of delta growth. We introduce a list of all the state variables with their dimensions in Table 1.

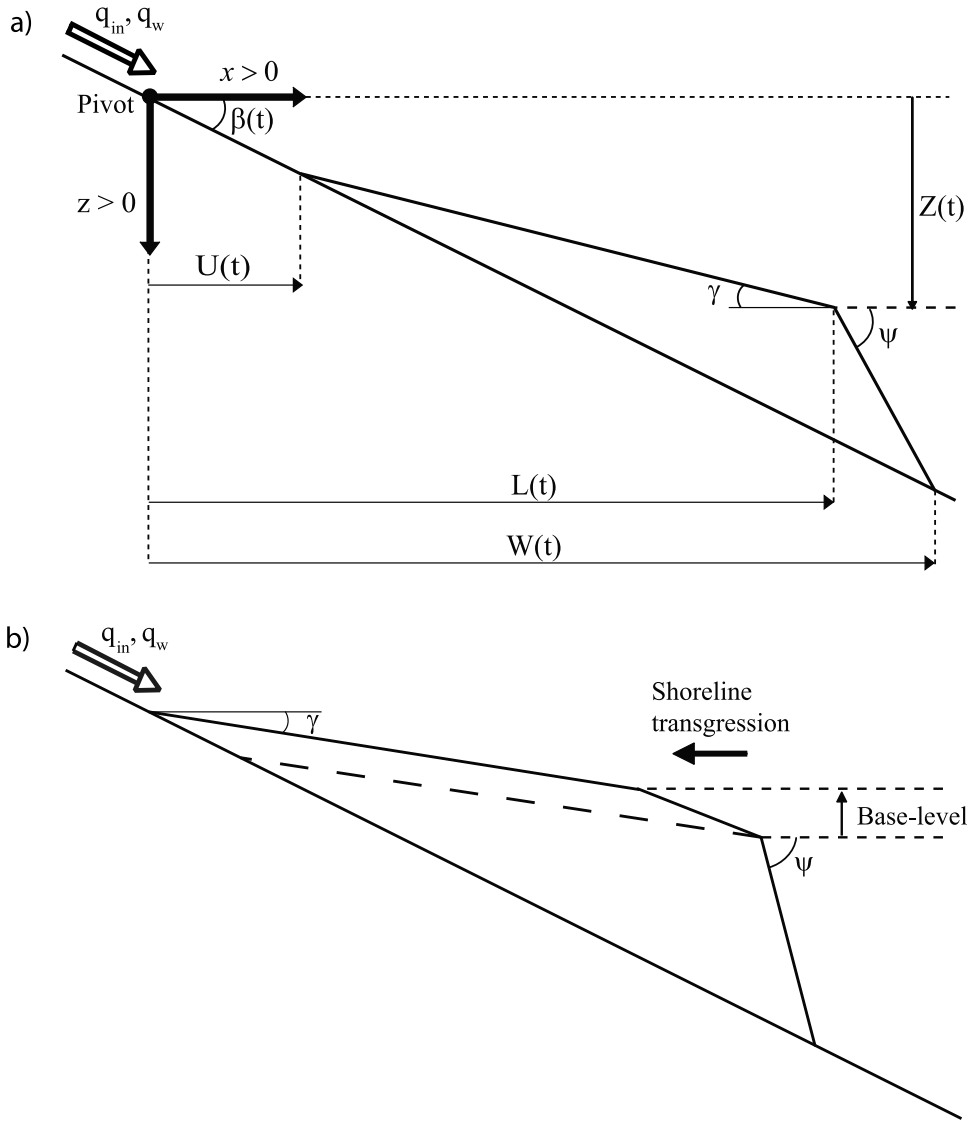

Figure 2. (a) Sketch including the state variables (see Table 1). (b) Deltaic system undergoing shoreline retreat.

[11] We are interested in modeling marine deltas, such as the Mississippi River Delta, that have a basement slope $\beta \sim 10^{-3} - 10^{-4}$ [*Kosters et al.*, 1987; *Blum and Törnqvist*, 2000; *Muto and Steel*, 2002; *Kim et al.*, 2009], a foreset slope $\psi \sim 10^{-2}$ [*Swenson et al.*, 2000; *Muto and Steel*, 2002], an average delta plain slope $\gamma \sim 10^{-5}$ [*Blum and Törnqvist*, 2000; *Blum and Roberts*, 2009], and a rate of sediment input ~100 Mton/year [*Kim et al.*, 2009]. Assuming a bulk density for the inorganic sediment input in the range 1.5–2 ton/m^3 [*Meckel et al.*, 2007] and a width of ~50–100 km the sediment input can be written as $q_{in} \sim$ 1000 m^2/year, which leads to an approximate time scale of $\tau \sim 1000$ years. The present base-level rise rate for the Mississippi River Delta area has been estimated to be $\dot{Z} \sim 7$ mm/year [*Kim et al.*, 2009; *Penland and Ramsey*, 1990], and data from typical Holocene peat-forming environments throughout the world suggest that the organic matter accumulation rate in the subsurface P can vary within the range 0–7 mm/year [*Diessel et al.*, 2000]. The value for organic matter accumulation is then poorly constrained, but in this first modeling exercise the objective is to explore the response under different values.

4. A Dimensionless Form

[12] A more general solution approach is achieved by casting (5) into a dimensionless form. Toward this end we use a characteristic basin length $\ell \sim 100$ km, and a time scale using the river sediment input $\tau = \ell^2 \beta_0 / q_{in}$. We identify the following dimensionless variables

$$L^d = \frac{L}{\ell}, \quad U^d = \frac{U}{\ell}, \quad Z^d = \frac{Z}{Z_0}, \quad V^d = \frac{V}{\ell^2 \beta_0} \tag{6a}$$

Table 1. State Variables and Their Dimensions

Symbol	Meaning	Dimensions (L, length, T time)
x	Horizontal distance positive in the downstream direction	L
z	Vertical distance positive downward	L
t	Time	T
V	Volume per unit width of the deltaic prism	L^2
q_{in}	River sediment flux into the deltaic system	L^2/T
L	Shoreline location	L
U	Alluvial-basement transition location	L
W	Delta toe location	L
χ	Thickness of organic sediment	L
$\dot{V}$	Rate of change of the volume per unit width of the deltaic prism	L^2/T
v_{org}	Rate of organic sedimentation	L/T
γ	Fluvial plain slope	-
β	Basement slope	-
β_0	Initial basement slope	-
$\dot{\beta}$	Rate of pivot subsidence	1/T
φ	Subaqueous foreset slope	-
Z	Base-level	L
Z_0	Initial base-level	L
$\dot{z}$	Rate of base-level rise	L/T
A	Rate of accommodation	L/T
P	Rate of organic matter accumulation	L/T

And the following dimensionless groups that specify the behavior of the system

$$\gamma^d = \frac{\gamma}{\beta_0}, \quad \psi^d = \frac{\psi}{\beta_0}, \quad \dot{Z}^d = \frac{\dot{Z}\ell}{q_{in}}, \quad \dot{\beta}^d = \frac{\dot{\beta}\ell^2}{q_{in}}, \quad P^d = \frac{P\ell}{q_{in}} \tag{6b}$$

With the definitions in (6), and dropping the d superscript for convenience of notation, the dimensionless governing equations under base-level rise and differential subsidence become

$$\dot{V} = 1 + (L - U) \cdot \min(\dot{Z}, P) \tag{7a}$$

$$\dot{V} = 1 + \int_U^L \min(\dot{\beta}x, P)dx \tag{7b}$$

where $\dot{V} = dV/dt$, and with initial conditions $V = 0$, $L = 1$, and $U = 1$. The dimensionless base-level Z and basement slope β are written as follows

$$Z = 1 - \dot{Z}t \tag{8a}$$

$$\beta = 1 + \dot{\beta}t \tag{8b}$$

We include a list of the dimensionless state variables in Table 2. Using the parameter values discussed in previous section, we constrain the dimensionless groups defined in (6b) as a reference for the following calculations. We note that the fluvial slope ratio is in the range $\gamma \sim 0.1$–0.01, which validates the linear fluvial slope assumption, and that the foreset slope ratio is typically very large ($\psi \gg 1$), implying that the sediment stored below the foreset is relatively very small and can be dropped without error from any volume balance calculation. The current dimensionless base-level rise rate in the Mississippi River Delta is $\dot{Z} \sim 0.7$, and the dimensionless organic matter accumulation rate in the range $P \sim 0 - 0.7$.

5. Model Solution

[13] At a given time $t > 0$, if the right hand side of (7) and the current volume of the delta deposit V^{old} are known, the value of the volume V at a small increment of time Δt beyond time t can be calculated with a simple Euler scheme

$$V = V^{old} + \Delta t \dot{V} \tag{9}$$

where $\dot{V}$ is given by (7). The integral on the right hand side of (7b) is estimated numerically using a simple trapezoidal rule

$$\int_U^L \min(\dot{\beta}x, P)dx \approx \frac{L - U}{2N} \sum_{k=1}^{N} \left(\min(\dot{\beta}x_{k+1}, P) + \min(\dot{\beta}x_k, P) \right) \tag{10}$$

where $N + 1$ is the number of equally spaced grid points.

[14] In order to define the delta profile evolution and to generate the information to complete subsequent time steps

Table 2. State Dimensionless Variables Described in Equations (6), (7), (8), (12), (13), and (14)[a]

Symbol	Meaning
x	Horizontal distance positive in the seaward direction
z	Vertical distance positive downward
t	Time
V	Volume per unit width of the deltaic prism
L	Shoreline location
U	Alluvial-basement transition location
W	Delta toe location
$\dot{V}$	Rate of change of the volume per unit width of the deltaic prism
v_{in}	Rate of inorganic sedimentation
$(v_{in})_{dp}$	Rate of inorganic sedimentation that exceeds the accommodation rate and is trapped within the delta plain
v_{org}	Dimensionless rate of organic sedimentation
γ	Fluvial plain slope
β	Basement slope
$\dot{\beta}$	Rate of pivot subsidence
φ	Subaqueous foreset slope
Z	Base-level
$\dot{z}$	Rate of base-level rise
A	Rate of accommodation
P	Rate of organic matter accumulation
P_f	Rate of organic matter accumulation in fresh water environments
F	Length of the fresh water environments
P_s	Rate of organic matter accumulation in saline environments
S	Length of saline environments
K	Fraction of the delta plain with saline ecosystems
t^*	Time of conversion from fresh to saline environments
C_f	Organic fraction

[a]Note that for convenience of notation they share symbol with the state variables with dimensions introduced in Table 1.

Table 3. Geometric Relationships for the Base-Level Rise Scenario[a]

	Shoreline Advance	Shoreline Retreat
Shoreline increment	WHILE $\Delta L = \sqrt{2V(1-\gamma)} + Z - L^{old} \geq 0$	ELSE UNTIL $\Delta L = \frac{\Delta t}{\gamma}\left(\frac{\dot{V}}{L-U} - \dot{Z}\right) < 0$
Shoreline position	$L = L^{old} + \Delta L$	
Alluvial-basement transition position	$U = Z - \gamma\sqrt{\frac{2V}{1-\gamma}}$	$U = \frac{Z-\gamma L}{1-\gamma}$

[a]The value of Z is obtained from equation (2a).

calculations we need a means of extracting the positions of the alluvial-basement transition $U(t)$ and the shoreline $L(t)$ from this updated value of the total volume, V. In Tables 3 and 4 we include a list of the relevant calculation steps to achieve this; all the expressions are derived from direct geometric arguments.

[15] The calculation requires three input parameters: the slope ratio γ, the organic matter accumulation rate P, and either the base-level rise rate $\dot{Z}$ or the pivot subsidence rate $\dot{\beta}$. In operation, following the update of the volume V from (9) we first calculate the shoreline change increment within a time step ΔL and then the shoreline and alluvial-basement transition positions L and U. If the shoreline moves seawards (i.e., $\Delta L \geq 0$), we follow the calculations on the left column in Tables 3 and 4. At some point in the calculation, however, the sediment supply and the organic matter accumulation cannot sustain a shoreline advance causing a shoreline retreat indicated by an estimated value $\Delta L < 0$. In this case we switch to the expressions in the right column in Tables 3 and 4. In connecting to previous models, we note that if the organic matter accumulation rate is zeroed out, i.e., $P = 0$, the model presented in Table 3 recovers the previous model developed by *Kim and Muto* [2007].

[16] In Figure 3 we present the typical model behavior under constant base-level rise (Table3). We choose a base-level rise rate $\dot{Z} = 0.8$, a the slope ratio $\gamma = 0.01$, and an organic matter accumulation rate $P = 0.4$. Initially the total rate of sediment input $\dot{V}$ exceeds the total accommodation rate in the delta plain $\dot{Z}(L - U)$, and, as depicted in Figure 3, the shoreline trajectory moves seawards $\Delta L > 0$. As time increases the delta length $(L - U)$ increases monotonically and at some point in time cannot be maintained by the sediment input, which leads to shoreline retreat, i.e., $\Delta L < 0$. Both the alluvial-basement transition and the shoreline reach a constant landwards speed $\Delta U/\Delta t = \Delta L/\Delta t = -\dot{Z}$ and the delta length reaches a steady value $(L - U) = 1/((1 - \gamma)\dot{Z} - \min(\dot{Z}, P))$.

[17] In Figure 4 we present the typical model behavior under pivot subsidence (Table 4). We use two subsidence rates: $\dot{\beta} = 2.2$ (solid lines) and $\dot{\beta} = 2.8$ (dashed lines). The slope ratio is $\gamma = 0.01$, and the organic matter accumulation rate is $P = 0.4$. Initially, similarly to the base-level rise scenario, the total rate of sediment input $\dot{V}$ exceeds the total accommodation rate $\dot{\beta}(L + U)/2$, and, as depicted in Figure 4, the shoreline trajectory moves seawards $\Delta L > 0$. At later stages of delta growth, however, the shoreline can have two possible behaviors: (1) it can monotonically approach a steady location (solid line), or (2), it can overshoot and retreat before reaching the steady location (dashed line). The shoreline reaches the steady location and the delta length reaches a steady value when the sediment input rate balances accommodation rate: at this point the alluvial-basement transition is fixed at the pivot location (see Figure 5).

[18] We note that the behaviors depicted in Figures 3 and 4 apply for any set of parameter values γ, P, $\dot{Z}$, and $\dot{\beta}$ as long as the accommodation rate is positive and finite (i.e., $\dot{Z} > 0$ or $\dot{\beta} > 0$).

6. Calculating Organic Fraction

[19] A simple and worthwhile extension of the model presented above is to calculate the organic fraction C_f, defined as the ratio between the organic and total (i.e., organic and inorganic) sediment volume in the sediment column. We define the average organic fraction in the time interval (t_1, t_2) at a given location x in the delta plain in terms of the organic v_{org} and inorganic v_{in} sedimentation rates as follows

$$C_f(x) = \frac{\sum_{t_1}^{t_2} v_{org}(x)\Delta t}{\sum_{t_1}^{t_2} \left(v_{org}(x) + v_{in}(x)\right)\Delta t} \tag{11}$$

The organic sedimentation v_{org} is described in equation (4). The inorganic sedimentation v_{in} first fills the fraction of the accommodation A not occupied by organics, and the excess (if any) is distributed between the delta plain and the subaqueous foreset. Since the accommodation rate A is constant in time for the base-level rise $A = \dot{Z}$ and differential subsidence $A = \dot{\beta}x$ scenarios, we can write (11) as follows

$$C_f = \frac{\min(A, P)(t_2 - t_1)}{A(t_2 - t_1) + \sum_{t_1}^{t_2} (v_{in})_{dp}\Delta t} \tag{12a}$$

Table 4. Geometric Relationships for the Pivot Subsidence Scenario[a]

	Shoreline Advance	Shoreline Retreat
Shoreline increment	WHILE $\Delta L = \frac{\sqrt{2V(\beta-\gamma)}}{\beta} + \frac{1}{\beta} - L^{old} \geq 0$	ELSE UNTIL $\Delta L = \frac{\Delta t}{\gamma}\left[\frac{\dot{V}}{L-U} - \frac{\dot{\beta}}{2}(L+U)\right] \geq 0$
Shoreline position	$L = L^{old} + \Delta L$	
Alluvial-basement transition position	$U = \frac{1}{\beta} - \frac{\gamma}{\beta}\sqrt{\frac{2V}{\beta-\gamma}}$	$U = \frac{1-\gamma L}{\beta-\gamma}$

[a]The value of β is obtained from equation (2b).

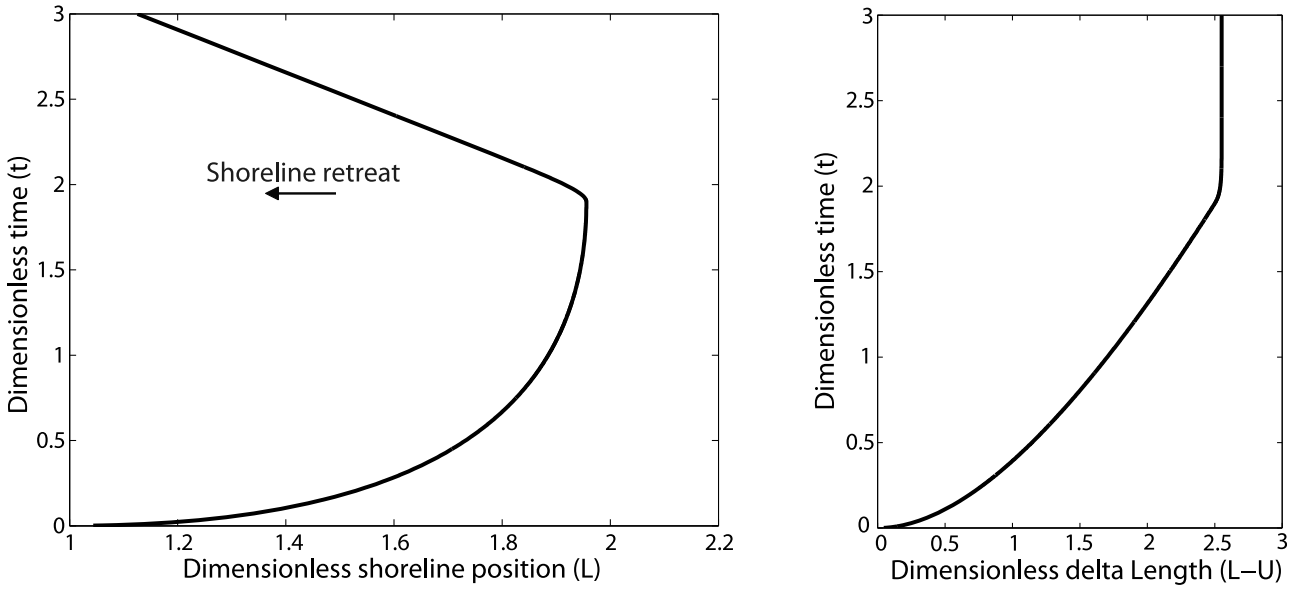

Figure 3. System response under steady base-level rise and constant organic matter accumulation rate *P*. We include (left) the shoreline position over time and (right) the delta length over time. Initially the sediment input fills the accommodation and the excess drives shoreline progradation. At some point in time the sediment supply becomes insufficient to fill the accommodation and the shoreline abandons the delta front and retreats.

where $(v_{in})_{dp}$ is the excess of inorganic sediments retained in the delta plain. We exclude the excess that accumulate in the foreset; an approach consistent with how measurements are made in the field, which only consider the organic-rich sections of any given core [*Bohacs and Suter*, 1997; *Diessel et al.*, 2000]. During shoreline advance $\Delta L \leq 0$, $(v_{in})_{dp}$ is obtained through geometric construction, and during shoreline retreat $\Delta L \leq 0$ the entire inorganic sediment supply is

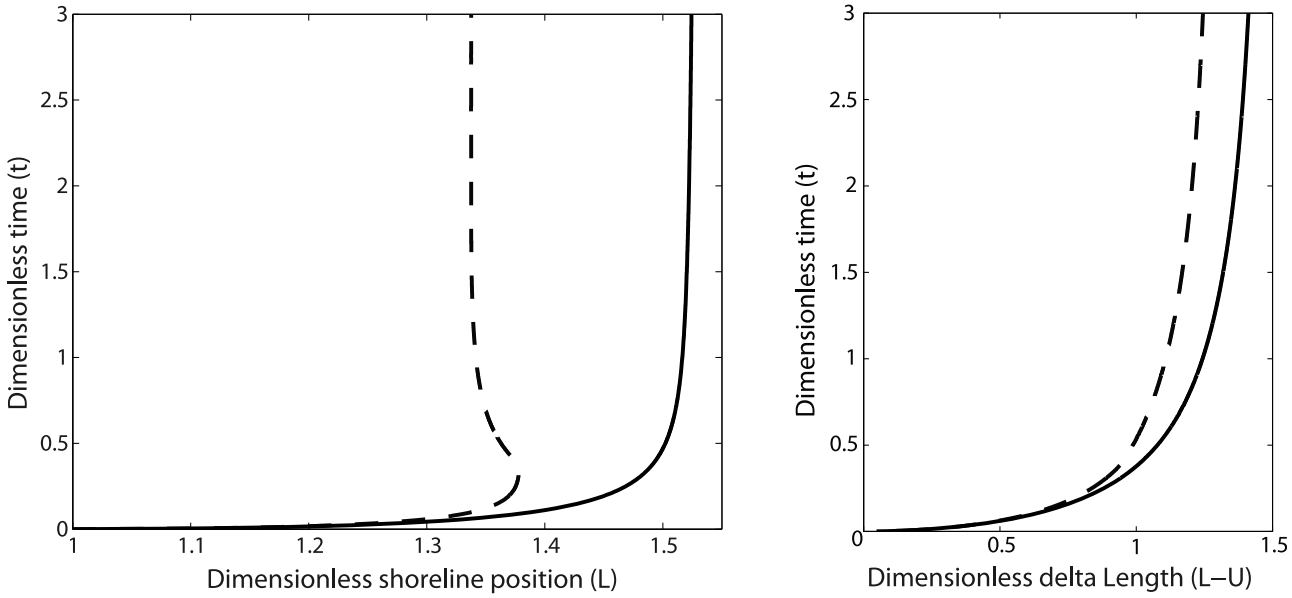

Figure 4. System response under low (solid line) and high (dashed line) pivot subsidence rates, and constant organic matter accumulation rate *P*. We include (left) the shoreline position over time and (right) the delta length over time. Under slow subsidence, the shoreline and the alluvial basement transition monotonically approach a steady location where the sediment input matches the accommodation rate (see Figure 5). Under fast subsidence rate the shoreline overshoots and retreats before reaching the steady location.

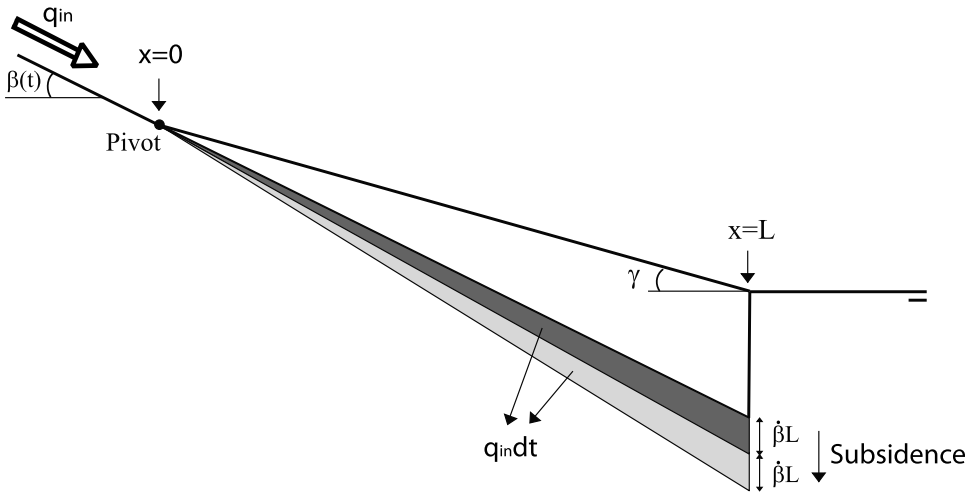

Figure 5. System equilibrium for the pivot subsidence scenario where the sediment input matches the accommodation rate and both the alluvial basement transition and the shoreline are at steady locations.

included in the accommodation term A. We can then write it as follows

$$(v_{in})_{dp} = \begin{cases} \gamma \Delta L/\Delta t & \Delta L > 0 \\ 0 & \Delta L \le 0 \end{cases} \qquad (12b)$$

7. Comparison With Coal and Peat Data

[20] Coal geologists have observed that the fundamental control of the organic fraction in the sediment column C_f is the ratio between accommodation rate A (space made for sediment accumulation) and organic matter accumulation rate P. [*Bohacs and Suter*, 1997; *Diessel et al.*, 2000].

[21] Here we assume P to be a constant value, an assumption that will be relaxed in the next section. In the base-level rise scenario, the accommodation rate $A = \dot{Z}$ is also a constant. Thus, substituting $A = \dot{Z}$ and P into equation (12) we obtain a constant organic fraction C_f along the delta plain. In Figure 6 we plot the organic fraction as a function of the ratio $\dot{Z}/P$ for the input parameters indicated. A key observation, independent of the parameter values chosen, is the occurrence of a maximum organic fraction when the accommodation rate matches the organic matter accumulation rate, i.e., $\dot{Z}/P = 1$. This result matches the widely made observation in the coal literature of maximum peat fractions in systems where organic matter accumulation rate matches the accommodation rate, i.e., $\dot{Z}/P \sim 1$ [*Bohacs and Suter*, 1997; *Diessel et al.*, 2000]. We also include the range for coal accumulation (i.e., $C_f > 0.75$), and note that the model recovers within a narrow range the upper limit previously obtained by *Bohacs and Suter* [1997] (i.e., $\dot{Z}/P = 1.18$). The lower limit for coal accumulation, however, is lower than what is typically observed in the field [*Bohacs and Suter*, 1997; *Diessel et al.*, 2000] and more sensitive to the input parameters. Future work will study the sensitivity of the coal accumulation range in more detail.

[22] Under differential subsidence, both the accommodation rate $A = \dot{\beta}x$ and the organic fraction C_f are functions of location on the delta plain x. In Figures 7 and 8 we plot the organic fraction as a function of $A/P = (\dot{\beta}/P)x$. In Figure 7 we vary the ratio $\dot{\beta}/P$ and fix the location at $x = 1$, whereas in Figure 8 we vary the location x and fix the ratio $\dot{\beta}/P$. Again, the key observations are: (1) the occurrence of the maximum organic fraction when the accommodation rate matches the organic matter accumulation rate $A/P = 1$ [*Bohacs and Suter*, 1997; *Diessel et al.*, 2000], and (2) the upper limit for coal accumulation that emerges from the model matches within a narrow range the result obtained by *Bohacs and Suter* [1997].

[23] We view these results as a validation of our modeling approach, in particular our assumption of fluvial shape preservation that constrains the organic sedimentation to be

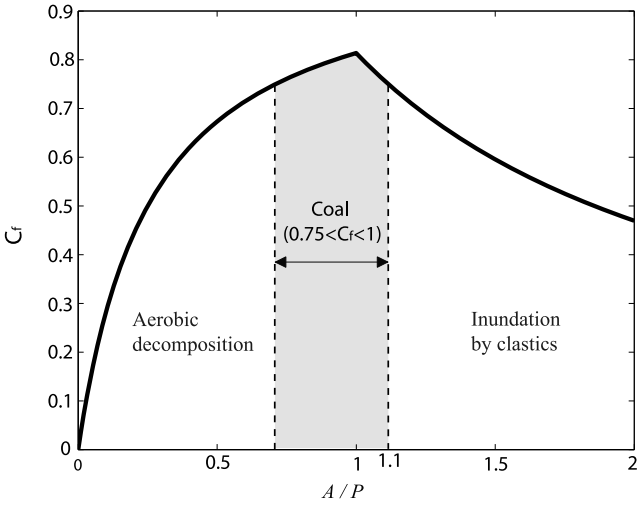

Figure 6. Plot of the organic fraction C_f as a function of the ratio $A/P = \dot{Z}/P$. The slope ratio is $\gamma = 0.1$, the running time $t = 3$, and the time interval for the organic fraction calculation is $(t_1, t_2) = (0, 3)$. The region in gray corresponds to values of C_f at which coal accumulation is possible [*Bohacs and Suter*, 1997].

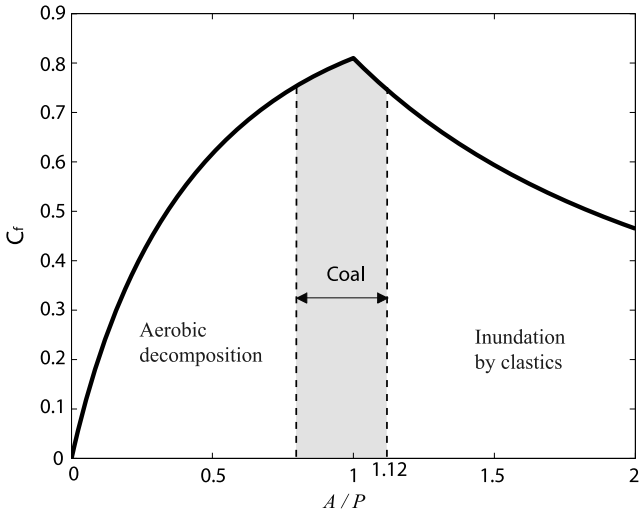

Figure 7. Plot of the organic fraction C_f as a function of $A/P = (\dot{\beta}/P)x$ at a fixed location $x = 1$. We also fix the slope ratio $\gamma = 0.2$, the running time $t = 5$, and the time interval for the organic fraction calculation $(t_1, t_2) = (0, 5)$. The region in gray corresponds to values of C_f at which coal accumulation is possible [*Bohacs and Suter*, 1997].

the minimum of the organic matter accumulation rate P and accommodation rate A (equation (4)).

8. The Role of the Fresh-Salt Boundary Dynamic in Delta Evolution

[24] In the initial derivation and application of our model we have assumed a constant value for the organic matter accumulation rate P. We now generalize this assumption by accounting for the potentially important effects of different organic matter accumulation rates between saline and fresh environments (see discussion in section 2). On deltaic coasts, several factors control the extent of the fresh water region such as the fresh water supply, precipitation intensity, base-level fluctuations, and topography, but numerical modeling and field studies in the Ebro delta point out the fresh water inputs from the river as the main control [*Ibañez et al.*, 1997; *Sierra et al.*, 2004]. A reduction in the river water supply leads to saltwater intrusion, which accelerates the decomposition of organic soils due to the shift in anaerobic respiration from methanogesis to sulfate reduction [*Capone and Kiene*, 1988; *Portnoy and Giblin*, 1997; *Portnoy*, 1999; *Ibañez et al.*, 2010]. Human activities such as channelization play a key role in controlling the fresh water supply [*Day et al.*, 1997; *Williams et al.*, 1999; *Sierra et al.*, 2004]. Additionally, changes in water supply on centennial to millennial time scales can be caused naturally by climate change or an abandonment of the river channel. Paleoflood chronologies from the Mississippi river have been used to conclude that minor changes in climate can produce very high changes in water discharge [*Knox*, 1993].

[25] To illustrate how our model can be generalized to account for spatial variations in organic matter accumulation controlled by changes in fresh-water inputs, we consider a scenario of a delta initially in a purely freshwater environment that at some time t^* converts to a delta that contains both a fresh region of length f and a saline region of length s. This transition is taken to be instantaneous, i.e., short compared to the time scale of delta response. This example does not intend to model any system in particular, but aims to explore the importance of the fresh-salt transition on delta evolution. If we denote organic matter accumulation rate in the fresh region by P_f and in the saline region by P_s, a modified form of the governing equation in (7) can be written as

$$\dot{V} = 1 + \int_{U}^{U+f} \min(A, P_f)\, dx + \int_{U+f}^{L} \min(A, P_s)\, dx \qquad (13)$$

which on specification of an appropriate relationship between f, s, L and U can be solved by a simple extension of the approach detailed in Tables 3 and 4. For the case under consideration these relationships are

$$f = \begin{cases} L - U & t < t^* \\ (1-k)(L-U) & t \geq t^* \end{cases} \qquad (14a)$$

$$f + s = L - U \qquad (14b)$$

where k is the fraction of the delta that is eventually under saline conditions.

[26] Under a steady base-level rise, an early shift of the fresh-salt transition modifies the time and the location at which the shoreline retreat begins (Figure 9a). When the delta is always fresh ($k = 0$), the shoreline advances farther and for a longer time period than a combined fresh/saline delta ($k = 0.5, 1$). In contrast, a shift in a more advanced stage of delta growth leads to an abrupt increase of the shoreline retreat speed (Figure 9b).

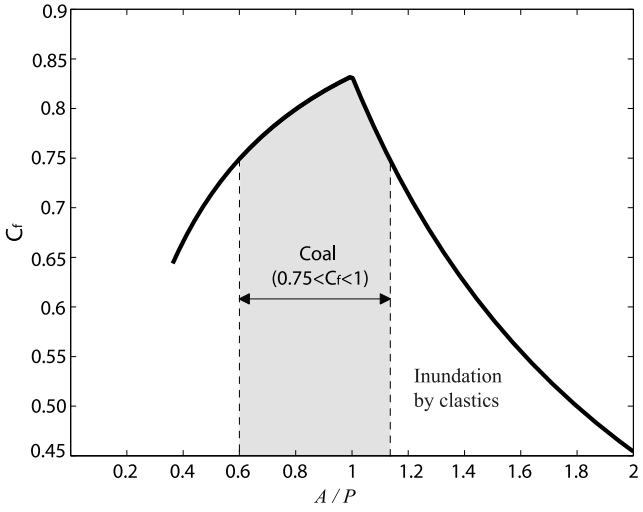

Figure 8. Plot of the organic fraction C_f as a function of $A/P = (\dot{\beta}/P)x$ for a fixed subsidence rate $\dot{\beta} = 0.3$, and organic matter accumulation rate $P = 0.3$. We also fix the slope ratio $\gamma = 0.2$, the running time $t = 3$, and the time interval for the organic fraction calculation $(t_1, t_2) = (1.5, 3)$. The region in gray corresponds to values of C_f at which coal accumulation is possible [*Bohacs and Suter*, 1997].

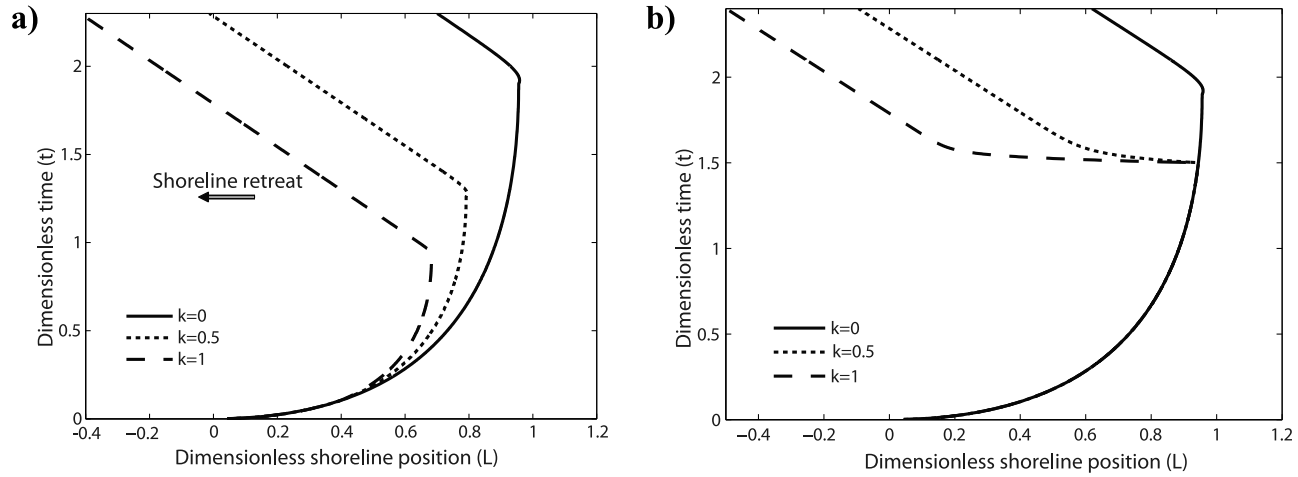

Figure 9. Shoreline response to a landwards shift of the fresh-salt transition and a steady base-level rise $\dot{Z} = 0.8$. The system is initially entirely fresh and at time (a) $t^* = 0.1$, and (b) $t^* = 1.5$, a fraction k of the delta plain becomes saline. The slope ratio is $\gamma = 0.01$, and the organic matter accumulation rates are $P_f = 0.4$, and $P_s = 0.1$.

[27] Similarly, under differential subsidence the fresh-salt transition shift can also lead to an abrupt increase of the shoreline retreat speed before reaching a steady location (Figure 10). Therefore, Figures 9 and 10 suggest that the extension of the fresh water region can potentially have a strong effect on shoreline dynamics. The higher organic matter accumulation in fresh water environments compared to saline environments implies that a reduction in fresh water inputs can lead to a rapid shoreline retreat. Episodes of punctuated shoreline retreat observed in the Gulf of Mexico, however, are usually interpreted as an increase in the rate of base-level rise [*Rodriguez et al.*, 2010], a reduction in river sediment input [*Milliken et al.*, 2008], or topography complexity [*Rodriguez et al.*, 2004, 2005]. We present the motion of the fresh-salt boundary as a potential candidate to explain (or amplify) this back stepping shoreline behavior.

9. Conclusions

[28] We present a simple geometric model that for the first time captures the basic interplay of organic and clastic deposition in deltas under base-level rise and differential subsidence. The model reproduces a central observation from coal geology, that organic fraction is maximized when the organic matter accumulation and accommodation rates are just balanced. The model also recovers the upper limit for potential coal accumulation predicted by *Bohacs and Suter* [1997]. Moreover, the model shows that the imbalance in organic sedimentation between fresh and saline environments can significantly alter delta evolution. In particular, a landwards shift of the fresh-salt transition caused by a reduction in fresh water inputs can lead to a punctuated shoreline retreat.

[29] A number of modifications will significantly improve the utility of the model presented here. In particular we plan to include a more complete mechanistic description of the movement of the fresh-salt boundary, which is currently assumed to be an input of the model. Additionally, we need to incorporate field and experimental data to better constrain the model parameters of organic matter accumulation P_f and P_s. These improvements will lead to a consistent mathematical framework for the characterization of the accretion/oxidation of organic soil in deltas. Such a tool can be used to advance existing modeling efforts pertaining to land building in the Mississippi River Delta [*Kim et al.*, 2009]. Additionally, we intend to use it to better understand the relative importance of variations of the fresh-salt boundary compared to variations on allogenic controls such as base-level or river sediment input. Future versions of the model will also aim to address current concerns related to the increase of nutrient supply into the wetland ecosystems of the Mississippi River Delta [*Perez et al.*, 2011]. Among other important effects, an

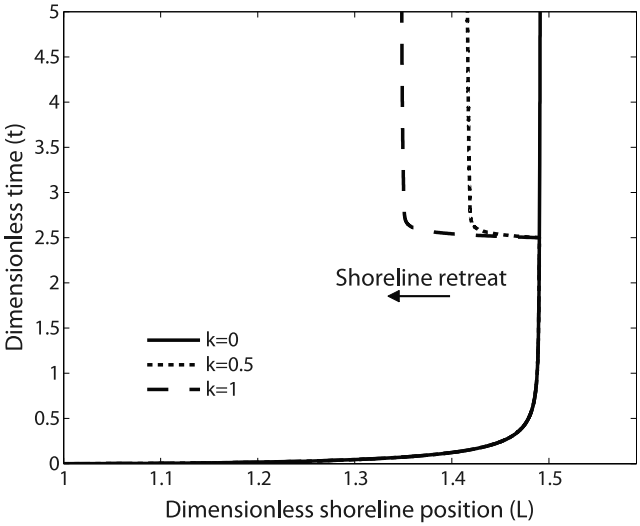

Figure 10. Shoreline response to a landwards shift of the fresh-salt transition and subsidence rate $\dot{\beta} = 2.3$. The system is initially entirely fresh and at time $t^* = 2.5$, a fraction k of the delta plain becomes saline. The slope ratio is $\gamma = 0.1$, and the organic matter accumulation rates are $P_f = 0.4$, and $P_s = 0.1$.

increase in nutrient concentration in river water can enhance decomposition and aboveground versus below-ground productivity [*Perez et al.*, 2011]. This can result in an increase in vulnerability of wetland vegetation, and thus, a decrease in long-term plant matter accumulation in the sediment column.

[30] **Acknowledgments.** We are grateful to the reviews from Kevin Bohacs, Torbjörn Törnqvist, Matt Kirwan, and Alexander Densmore which have helped to improve the clarity of the manuscript. This work was supported by the STC program of the National Science Foundation via the National Center for Earth-surface Dynamics under the agreement EAR-0120914.

References

Allison, M. A., S. A. Kuehl, T. C. Martin, and A. Hassan (1998), Importance of flood-plain sedimentation for river sediment budgets and terrigenous input to the oceans: Insights from the Brahmaputra-Jamuna River, *Geology*, *26*, 175–178, doi:10.1130/0091-7613(1998)026<0175:IOFPSF>2.3.CO;2.

Bianchi, T. S. (2011), The role of terrestrial derived organic carbon in the coastal ocean: A changing paradigm and the priming effect, *Proc. Natl. Acad. Sci. U. S. A.*, *108*(49), 19,473–19,481, doi:10.1073/pnas.1017982108.

Blum, M. D., and H. H. Roberts (2009), Drowning of the Mississippi Delta due to insufficient sediment supply and global sea-level rise, *Nat. Geosci.*, *2*(7), 488–491.

Blum, M. D., and T. E. Törnqvist (2000), Fluvial responses to climate and sea-level change: A review and look forward, *Sedimentology*, *47*, 2–48.

Bohacs, K. M., and J. Suter (1997), Sequence stratigraphic distribution of coaly rocks; fundamental controls and paralic examples, *AAPG Bull.*, *81*, 1612–1639.

Capart, H., M. Bellal, and D. L. Young (2007), Self-similar evolution of semi-infinite alluvial channels with moving boundaries, *J. Sediment. Res.*, *77*, 13–22, doi:10.2110/jsr.2007.009.

Capone, D. G., and R. P. Kiene (1988), Comparison of microbial dynamics in marine and freshwater sediments: Contrasts in anaerobic carbon catabolism, *Limnol. Oceanogr.*, *33*, 725–749, doi:10.4319/lo.1988.33.4_part_2.0725.

Clymo, R. S. (1983), Peat, in *Mires: Swamp, Bog, Fen and Moor, General Studies, Ecosyst. of the World*, vol. 4, edited by A. J. P. Gore, pp. 159–224, Elsevier, Amsterdam.

Costanza, R., et al. (1997), The value of the world's ecosystem services and natural capital, *Nature*, *387*, 253–260, doi:10.1038/387253a0.

Day, J. W., J. F. Martin, L. Cardoch, and P. H. Templet (1997), System functioning as a basis for sustainable management of deltaic ecosystems, *Coast. Manage.*, *25*(2), 115–153.

Diessel, C., R. Boyd, J. Wadsworth, D. Leckie, and G. Chalmers (2000), On balanced and unbalanced accommodation/peat accumulation ratios in the Cretaceous coals from Gates Formation, Western Canada, and their sequence-stratigraphic significance, *Int. J. Coal Geol.*, *43*, 143–186, doi:10.1016/S0166-5162(99)00058-0.

Fisk, H. N. (1960), Recent Mississippi River sedimentation and peat accumulation, in *Congres pur l'avancement des etudes de stratigraphie et de geologie du Carbonifiere*, pp. 187–199, Compte Rendu, Heerlen, Netherlands.

Gambolati, G., M. Putti, P. Teatini, and G. Gasparetto Stori (2006), Subsidence due to peat oxidation and impact on drainage infrastructures in a farmland catchment south of the Venice Lagoon, *Environ. Geol.*, *49*, 814–820, doi:10.1007/s00254-006-0176-6.

Howarth, R. W. (1984), The ecological significance of sulfur in the energy dynamics of salt marsh and coastal marine sediments, *Biogeochemistry*, *1*, 5–27, doi:10.1007/BF02181118.

Howarth, R. W., and J. E. Hobbie (1982), The regulation of decomposition and heterotrophic microbial activity in salt marsh soils: A review, in *Estuarine Comparisons*, edited by V. S. Kennedy, pp. 183–207, Academic Press, New York.

Ibañez, C., D. Pont, and N. Prat (1997), Characterization of the Ebre and Rhone estuaries: A basis for defining and classifying salt-wedge estuaries, *Limnol. Oceanogr.*, *42*, 89–101, doi:10.4319/lo.1997.42.1.0089.

Ibañez, C., P. J. Sharpe, J. W. Day, J. N. Day, and N. Prat (2010), Vertical accretion and relative sea-level rise in the Ebro delta wetlands, *Wetlands*, *30*, 979–988, doi:10.1007/s13157-010-0092-0.

Kim, W., and T. Muto (2007), Autogenic response of alluvial-bedrock transition to base-level variation: Experiment and theory, *J. Geophys. Res.*, *112*, F03S14, doi:10.1029/2006JF000561.

Kim, W., D. Mohrig, R. Twilley, C. Paola, and G. Parker (2009), Is It feasible to build new land in the Mississippi River delta?, *Eos Trans. AGU*, *90*, 373–374, doi:10.1029/2009EO420001.

Kirwan, M. L., and A. B. Murray (2007), A coupled geomorphic end ecological model of tidal marsh evolution, *Proc. Natl. Acad. Sci. U. S. A.*, *104*, 6118–6122, doi:10.1073/pnas.0700958104.

Knox, J. C. (1993), Large increases in flood magnitude in response to modest changes in climate, *Nature*, *361*, 430–432, doi:10.1038/361430a0.

Kosters, E. C., and J. R. Suter (1993), Facies relationship and system tracts in the late Holocene Mississippi delta plain, *J. Sediment. Petrol.*, *63*, 727–733.

Kosters, E. C., G. L. Chmura, and A. Bailey (1987), Sedimentary and botanical factors influencing peat accumulation in the Mississippi Delta, *J. Geol. Soc.*, *144*, 423–434, doi:10.1144/gsjgs.144.3.0423.

Long, A. J., M. P. Waller, and P. Stupples (2006), Driving mechanisms of coastal change: Peat compaction and the destruction of late Holocene coastal wetlands, *Mar. Geol.*, *225*, 63–84, doi:10.1016/j.margeo.2005.09.004.

Lorenzo-Trueba, J., and V. R. Voller (2010), Analytical and numerical solution of a generalized Stefan problem exhibiting two moving boundaries with application to ocean delta formation, *J. Math. Anal. Appl.*, *366*, 538–549, doi:10.1016/j.jmaa.2010.01.008.

Lorenzo-Trueba, J., V. R. Voller, T. Muto, W. Kim, C. Paola, and J. B. Swenson (2009), A similarity solution for a dual moving boundary problem associated with a coastal-plain depositional system, *J. Fluid Mech.*, *628*, 427–443, doi:10.1017/S0022112009006715.

Meckel, T. A., U. S. Ten Brink, and S. J. Williams (2007), Sediment compaction rates and subsidence in deltaic plains: Numerical constraints and stratigraphic influences, *Basin Res.*, *19*, 19–31, doi:10.1111/j.1365-2117.2006.00310.x.

Milliken, K. T., J. B. Anderson, and A. B. Rodriguez (2008), Tracking the Holocene evolution of Sabine Lake through the interplay of eustasy, antecedent topography, and sediment supply variations, Texas and Louisiana, USA, *Spec. Pap. Geol. Soc. Am.*, *443*, 65–88, doi:10.1130/2008.2443(05).

Moore, P. D. (1989), The ecology of peat-forming processes: A review, *Int. J. Coal Geol.*, *12*, 89–103, doi:10.1016/0166-5162(89)90048-7.

Morris, J. T., P. V. Sundareshwar, C. T. Nietch, B. Kjerfve, and D. R. Cahoon (2002), Responses of coastal wetlands to rising sea level, *Ecology*, *83*(10), 2869–2877.

Muto, T., and R. J. Steel (2002), In defense of shelf-edge delta development during falling and lowstand of relative sea level, *J. Geol.*, *110*, 421–436, doi:10.1086/340631.

Mudd, S. M., S. M. Howell, and J. T. Morris (2009), Impact of dynamic feedbacks between sedimentation, sea-level rise, and biomass production on near-surface marsh stratigraphy and carbon accumulation, *Estuarine Coastal Shelf Sci.*, *82*(3), 377–389.

Paola, C., R. R. Twilley, D. A. Edmonds, W. Kim, D. Mohrig, G. Parker, E. Viparelli, and V. R. Voller (2011), Natural processes in delta restoration: Application to the Mississippi Delta, *Annu. Rev. Mar. Sci.*, *3*, 67–91, doi:10.1146/annurev-marine-120709-142856.

Parker, G., T. Muto, Y. Akamatsu, W. E. Dietrich, and J. W. Lauer (2008a), Unraveling the conundrum of river response to rising sea- level from laboratory to field, Part I: Laboratory experiments, *Sedimentology*, *55*, 1643–1655, doi:10.1111/j.1365-3091.2008.00961.x.

Parker, G., T. Muto, Y. Akamatsu, W. E. Dietrich, and J. W. Lauer (2008b), Unravelling the conundrum of river response to rising sea- level from laboratory to field, Part II. The Fly Strickland River system, Papua New Guinea, *Sedimentology*, *55*, 1657–1686, doi:10.1111/j.1365-3091.2008.00962.x.

Penland, S., and K. E. Ramsey (1990), Relative sea-level rise in Louisiana and the Gulf of Mexico: 1908–1988, *J. Coastal Res.*, *6*(2), 323–342.

Perez, B. C., J. W. Day, D. Justic, R. R. Lane, and R. R. Twilley (2011), Nutrient stoichiometry, freshwater residence time, and nutrient retention in a river-dominated estuary in the Mississippi Delta, *Hydrobiologia*, *658*(1), 41–54, doi:10.1007/s10750-010-0472-8.

Portnoy, J. W. (1999), Salt marsh diking and restoration: Biochemical implications of altered wetland hydrology, *Environ. Manage. N. Y.*, *24*, 111–120, doi:10.1007/s002679900219.

Portnoy, J. W., and A. E. Giblin (1997), Biogeochemical effects of seawater restoration to diked salt marshes, *Ecol. Appl.*, *7*, 1054–1063, doi:10.1890/1051-0761(1997)007[1054:BEOSRT]2.0.CO;2.

Reddy, R., and R. D. DeLaune (2008), *Biogeochemistry of Wetlands: Science and Applications*, CRC Press, Boca Raton, Fla., doi:10.1201/9780203491454.

Richardson, J. L., and M. J. Vepraskas (Eds.) (2001), *Wetland soils: Genesis, Hydrology, Landscapes, and Classification*, CRC Press, Boca Raton, Fla.

Rodriguez, A. B., J. B. Anderson, F. P. Siringan, and M. Taviani (2004), Holocene evolution of the East Texas coast and inner continental shelf: Along-strike variability in coastal retreat rates, *J. Sediment. Res.*, *74*(3), 405–421, doi:10.1306/092403740405.

Rodriguez, A. B., J. B. Anderson, and A. R. Simms (2005), Terrace inundation as an autocyclic mechanism for parasequence formation: Galveston

estuary, Texas, U.S.A, *J. Sediment. Res.*, *75*(4), 608–620, doi:10.2110/jsr.2005.050.

Rodriguez, A. B., A. R. Simms, and J. B. Anderson (2010), Bay-head deltas across the northern Gulf of Mexico back step in response to the 8.2 ka cooling event, *Quat. Sci. Rev.*, *29*, 3983–3993, doi:10.1016/j.quascirev.2010.10.004.

Sampere, T. P., T. S. Bianchi, M. A. Allison, and B. A. McKee (2011), Burial and degradation of organic carbon in Louisiana shelf/slope sediments, *Estuarine Coastal Shelf Sci.*, *95*(1), 232–244, doi:10.1016/j.ecss.2011.09.003.

Senior, E., E. B. Lindstrom, I. M. Banat, and D. B. Nedwell (1982), Sulfate reduction and methanogenesis in the sediment of a salt marsh on the East coast of the United-Kingdom, *Appl. Environ. Microbiol.*, *43*(5), 987–996.

Sierra, J. P., A. Sánchez-Arcilla, P. A. Figueras, J. González del Río, E. K. Rassmussen, and C. Mösso (2004), Effects of discharge reductions on salt wedge dynamics of Ebro river, *River Res. Appl.*, *20*, 61–77, doi:10.1002/rra.721.

Staub, J. R., and J. S. Esterle (1994), Peat-accumulating depositional systems of Sarawak, East Malaysia, *Sediment. Geol.*, *89*, 91–106, doi:10.1016/0037-0738(94)90085-X.

Swenson, J. B., C. Paola, G. Parker, and J. G. Marr (2000), Fluvio-deltaic sedimentation: A generalized Stefan problem, *Eur. J. Appl. Math.*, *11*, 433–452, doi:10.1017/S0956792500004198.

Törnqvist, T. E., D. J. Wallace, J. E. A. Storms, J. Wallinga, R. L. Dam, M. Blaauw, M. S. Derksen, C. J. W. Klerks, C. Meijneken, and E. M. A. Snijders (2008), Mississippi Delta subsidence primarily caused by compaction of Holocene strata, *Nat. Geosci.*, *1*, 173–176, doi:10.1038/ngeo129.

van Asselen, S. (2011), The contribution of peat compaction to total basin subsidence: Implications for the provision of accommodation space in organic-rich deltas, *Basin Res.*, *23*, 239–255, doi:10.1111/j.1365-2117.2010.00482.x.

van Asselen, S., E. Stouthamer, and T. van Asch (2009), Effects of peat compaction on delta evolution: A review on processes, responses, measuring and modeling, *Earth Sci. Rev.*, *92*, 35–51, doi:10.1016/j.earscirev.2008.11.001.

Williams, K., Z. S. Pinzon, R. P. Stumpf, and E. A. Raabe (1999), Sea-level Rise and Coastal Forests on the Gulf of Mexico, *U.S. Geol. Surv. Open File Rep.*, *99-441*, 127 pp.